



The utility of asymmetric flow field-flow fractionation for preclinical characterization of nanomedicines

Yingwen Hu¹ · Rachael M. Crist¹ · Jeffrey D. Clogston¹

Received: 18 September 2019 / Revised: 17 October 2019 / Accepted: 29 October 2019 / Published online: 27 November 2019
© Springer-Verlag GmbH Germany, part of Springer Nature 2019

Abstract

Dynamic light scattering (DLS), transmission electron microscopy (TEM), and reversed phase-high performance liquid chromatography (RP-HPLC) are staples of nanoparticle characterization for size distribution, shape/morphology, and composition, respectively. These techniques are simple and provide important details on sample characteristics. However, DLS and TEM are routinely done in batch-mode, while RP-HPLC affords separation of components within the entire sample population, regardless of sample polydispersity. While batch-mode analysis is informative and should be a first-step analysis for any material, it may not be ideal for polydisperse formulations, such as many nanomedicines. Herein, we describe the utility of asymmetric flow field-flow fractionation (AF4) as a useful tool for a more thorough understanding of these inherently polydisperse materials. AF4 was coupled with in-line DLS for an enhanced separation and resolution of various size populations in a nanomaterial. Additionally, the various size populations were collected for offline analysis by TEM for an assessment of different shape populations, or RP-HPLC to provide a compositional analysis of each individual size population. This technique was also extended to assess nanoparticle stability, i.e., drug release, both in buffer and physiologically relevant matrix, as well as qualitatively evaluate the protein binding capacity of nanomedicines. Overall, AF4 is proven to be a very versatile technique and can provide a wealth of information on a material's polydispersity and stability. Moreover, the ability to conduct analysis in physiological matrices provides an advantage that many other routine analytical techniques do not.

Keywords Nanoparticles · Size distribution · Polydispersity · Protein binding · Stability · Drug release

Introduction

Nanoparticle size can be measured by many different methods, the most common being dynamic light scattering (DLS), which measures the hydrodynamic size and provides information on the overall size distribution and polydispersity of the formulation [1, 2]. DLS measurements can be made in either batch-mode or flow-mode. In batch-mode DLS, measurements are made on the stock sample solution, with or without dilution—this is the most common type of DLS analysis. However, batch-mode DLS measurements are not ideal for many samples, especially samples that are known to be

inherently polydisperse, as many nanoformulations are [3, 4]. In flow-mode DLS, size measurements are made following a separation technique, wherein DLS is used as a downstream detector. Flow-mode DLS is particularly useful for polydispersed samples, as the fractionation helps circumvent the resolution issues associated with batch-mode measurements [5, 6].

Asymmetric flow field-flow fractionation (AF4) is a separation method based on separation by size. The theory, sample measurement, and profile optimization for AF4, as well as a comparison to other chromatographic methods, have been reviewed previously [7–10]. In brief, a parabolic laminar flow profile is established within a thin channel. The upper channel wall is impermeable while the bottom channel wall consists of a permeable membrane, often referred to as the accumulation wall. The driving force for separation is an applied perpendicular field, or cross-flow. The cross-flow forces the particles towards the accumulation wall, while Brownian motion counters this force. Larger particles with lower diffusion rates equilibrate at positions near the accumulation wall and

✉ Jeffrey D. Clogston
Jeffrey.Clogston@nih.gov

¹ Nanotechnology Characterization Laboratory, Cancer Research Technology Program, Leidos Biomedical Research, Inc., Frederick National Laboratory for Cancer Research, Frederick, MD 21702, USA

experience a low velocity profile. In contrast, smaller particles reside further away from the accumulation wall and experience a higher velocity profile. Thus, smaller particles generally travel the channel faster and elute first. Typically, AF4 is coupled with downstream detectors such as ultraviolet-visible spectrophotometry (UV-Vis), refractive index (RI), multi-angle light scattering (MALS), and DLS to determine purity, radius of gyration, and hydrodynamic size. Such setups have been used to characterize a variety of nanotechnology platforms, including liposomes [11–13], polymeric nanoparticles [14, 15], colloidal gold nanoparticles [16, 17], and gold nanorods [18, 19].

AF4 can also be coupled with a variety of other analytical techniques not suitable for in-line (downstream) detection [7, 10]. Polydisperse formulations can first be separated by AF4 with suitable in-line detectors, and the fractionated populations collected for analysis off-line by the technique of interest. For example, additional information on the size, shape, and morphology of the fraction can be obtained from transmission electron microscopy (TEM) analysis of AF4 fractions [20, 21]. Drug loading is another important characteristic which benefits from an initial AF4 separation. Drug concentrations are typically measured using reversed phase-high performance liquid chromatography (RP-HPLC) with either UV-Vis or fluorescence detection depending on the drug's spectral properties. However, this too is typically measured on the stock sample solution (with dilution). For polydisperse nanoformulations, a batch-mode measurement of the drug loading (i.e., total drug concentration) may not be ideal for a complete understanding of the formulation. In this case, drug loading is better represented as the drug distribution across the various size populations present (i.e., the drug concentration within each size population). Although RP-HPLC drug quantitation cannot be performed in-line of AF4 because of the sample preparation requirements to release the drug from the nanoparticles (e.g., liposomes are typically lyophilized and reconstituted in a suitable organic solvent to release the drug), samples can be fractionated and analyzed offline by RP-HPLC. The AF4-DLS-RP-HPLC approach allows for evaluation of drug distribution as a function of size, and is only possible with the combined analysis of all three instruments. Analyzing a polydisperse formulation with AF4, DLS, and RP-HPLC as stand-alone techniques, while still informative, does not provide the same level of detail as this combined approach.

AF4 can also be extended to examine nanoparticle stability in the presence of plasma proteins. Analytical characterization in biological matrix is an essential preclinical characterization component for any formulation being developed for systemic administration. Yet, many analytical techniques to probe the physicochemical properties of a formulation are not amenable to analysis in plasma. The interaction of nanoformulations with plasma proteins is extremely complex and can

dramatically affect formulation stability and in vivo biodistribution properties. Using AF4, not only can the stability of the nanoformulation (i.e., drug encapsulation/retention) be explored, but the extent of protein interactions with nanoformulations can also be explored. By using AF4 coupled with in-line MALS and DLS detection, the radius of gyration (R_g) and hydrodynamic radius (R_h), respectively, can be measured, and in turn, used to calculate shape factors ($\rho = R_g/R_h$) [6, 7, 22, 23]. The comparison of nanoparticle shape factors before and after incubation in plasma can provide information on protein binding and can be a useful tool in envisaging the in vivo properties of the formulation.

In this paper, we present several case studies which outline the vast potential of AF4 as a characterization technique for nanomedicines. Specifically highlighted are AF4 coupled with in-line DLS to explore size distribution, AF4-DLS with offline TEM analysis for an assessment of shape distribution, AF4-DLS with offline RP-HPLC analysis for measurement of drug distribution and assessment of nanoparticle stability in human plasma, and AF4-MALS-DLS for evaluation of nanoparticle protein binding. The utility of each individual analytical technique is shown to be far superior when combined with the separation capacity of AF4, to afford an overall better understanding of polydisperse nanoformulations.

Experimental section

Nanoparticles

Micellar formulations of SN-38 [24] and daunorubicin [25] were generously donated by Intezyme Technologies, Inc. PEGylated gold nanorods were generously donated by Siva Therapeutics. The dual doxorubicin- and docetaxel-loaded liposomes were generously donated by Cureport, Inc. The commercial formulations of Doxil®, Onivyde®, and AmBisome® were purchased from the National Institutes of Health (NIH) pharmacy.

Human plasma

For plasma incubation studies, human plasma was collected from healthy volunteer donors under National Cancer Institute (NCI) at Frederick Protocol OH99-C-N046.

Batch-mode dynamic light scattering

Hydrodynamic diameters were measured using a Malvern Zetasizer Nano ZS instrument (Malvern, Westborough, MA) with back scattering detector (173°). Samples were measured in batch-mode at 25 °C, using a quartz microcuvette. A minimum of five measurements were made for each sample.

Asymmetric flow field-flow fractionation

The asymmetric flow field-flow fractionation (AF4) system consisted of an isocratic pump (G1310B, Agilent, Palo Alto, CA), well-plate autosampler (G1329A, Agilent, Palo Alto, CA), AF4 separation channel (Eclipse AF4 or Eclipse DualTec, Wyatt Technology, Santa Barbara, CA), MALS detector (DAWN HELEOS II, Wyatt Technology, Santa Barbara, CA), UV-Vis detector (G1315B, Agilent, Palo Alto, CA), and a DLS instrument (Zetasizer Nano ZS, Malvern, Westborough, MA). The separation channel had a length of 275 mm (long channel) and a 350 μm spacer. A 10 kDa regenerated cellulose membrane was used for all separations. This membrane was pre-treated with high concentrations of a bovine serum albumin (BSA) solution to minimize non-specific binding to the membrane surface, following recommendations of the manufacturer. The mobile phase was phosphate-buffered saline (PBS, SH3025602, Hyclone, Thermo Fisher, Waltham, MA), filtered through a 0.2- μm regenerated cellulose membrane prior to use. Chromatographic traces were monitored by DLS detection, MALS detection, and/or UV-Vis detection. For flow-mode DLS analysis, measurements were made in a quartz flow cell (ZEN0023, Malvern, Westborough, MA) and data was collected using Malvern Zetasizer software (v7.11). The intensity threshold was manually adjusted after each experiment to distinguish background noise from signal. These values were sample dependent; values are given in the figure legends. The detector flow was 1 mL/min and the injection volume was 100 μL for all samples. For all samples described below, fractions were collected manually based on the DLS signal and stored at 4 °C for further analysis.

Reversed phase-high pressure liquid chromatography

The chromatographic system consisted of a quaternary pump (VF-P20-A, Thermo Fisher, Waltham, MA), autosampler (VF-A10-A, Thermo Fisher, Waltham, MA), Zorbax 300SB-C18 column (4.6 mm ID \times 150 mm, 5 μm , Agilent, Palo Alto, CA), and diode array (VH-D10-A, Thermo Fisher, Waltham, MA) and fluorescence (VF-D51-A, Thermo Fisher, Waltham, MA) detectors. The mobile phase consisted of water/ acetonitrile (A/B, HPLC Grade, both with 0.14% (w/v) trifluoroacetic acid) at a flow rate of 1 mL/min. The injection volume was 40 μL , and the column temperature was 25 °C for all samples.

SN-38 micelle analysis

Stock micellar SN-38 formulations were prepared at 50 mg/mL total construct in cold saline (4 °C). Samples were then diluted 10-fold in PBS before batch-mode DLS and AF4 analysis. The AF4 elution profile employed is given in Table 1.

The chromatographic traces were monitored by DLS detection and UV-Vis at 210 nm.

PEGylated gold nanorod analysis

Stock PEGylated (10 kDa) gold nanorods (1.8 mg/mL gold concentration) were diluted 10-fold in PBS for batch-mode DLS and 20-fold in PBS before AF4 analysis. The AF4 elution profile employed is given in Table 2. The chromatographic traces were monitored by MALS and DLS detection.

For batch-mode TEM analysis, stock PEGylated gold nanorods were diluted 50-fold with ultrapure water, and 2.5 μL was applied to a glow discharged carbon-coated copper film grid (Electron Microscopy Sciences). The grid was blotted and allowed to air dry before imaging. Images were taken using a T-12 TEM (FEI) equipped with a LaB₆ thermionic gun at 120 keV acceleration voltage. The fractions from AF4 separation were used without further dilution for analysis by TEM as described above. Multiple 2.5 μL aliquots of each fraction were repeatedly applied to the TEM grid to effectively increase the nanoparticle sampling for imaging.

Doxorubicin and docetaxel liposome analysis

Stock doxorubicin and docetaxel samples (2 mg DXR, 3 mg DTX/mL) were diluted 10-fold in PBS before AF4 analysis. The AF4 elution profile employed is given in Table 3. The chromatographic trace was monitored by DLS detection. Peak fractions were collected, and fraction volumes measured, before drug content analysis by RP-HPLC.

For doxorubicin quantitation, the RP-HPLC elution gradient was 25% B for 4 min, ramp to 100% B in 8 min, hold at 100% B for 4 min, and ramp down to 25% B in 4 min. Doxorubicin was detected by fluorescence emission at 590 nm (488 nm excitation). Calibration standards (LC Labs, D-4000, lot DXR-110) were prepared in 25% (v/v) acetonitrile at concentrations ranging from 20–200 ng/mL. Stock injection samples were lyophilized and reconstituted with 25% (v/v) acetonitrile accordingly to dilute the sample within the calibration curve range. Typically, 10 μL stock injection sample was lyophilized and reconstituted with 25% (v/v) acetonitrile to yield a 2000-fold final dilution. Collected fractions were either diluted or concentrated accordingly to fall within the calibration curve range. Typically, collected peak fractions were concentrated by first lyophilizing the sample, then reconstituting accordingly.

For docetaxel quantitation, the RP-HPLC elution gradient was 50% B for 4 min, ramp to 100% B in 10 min, hold at 100% B for 10 min, and ramp down to 50% B in 3 min. Docetaxel was detected by UV-Vis at 227 nm. Calibration standards (LC Labs, D-1000, lot BDC-105) were prepared in 25% (v/v) acetonitrile at concentrations ranging from 1–100 $\mu\text{g/mL}$. Stock injection samples were lyophilized and

Table 1 AF4 method for the analysis of SN-38 micelles

Step	Δt (min)	Mode	V _x start (mL/min)	V _x end (mL/min)	Focus flow (mL/min)
1	2	Elution	1	1	-
2	2	Focus	-	-	1
3	5	Focus + inject	-	-	1
4	10	Focus	-	-	1
5	10	Elution	1	1	-
6	2	Elution	1	0.5	-
7	10	Elution	0.5	0	-
8	20	Elution	0	0	-
9	2	Elution + inject	0	0	-
10	3	Elution	0	0	-

reconstituted with 25% (v/v) acetonitrile accordingly to fall within the calibration curve range. Typically, 20 μ L stock injection sample was lyophilized and reconstituted with 140 μ L 25% (v/v) acetonitrile to yield a 7-fold diluted sample. Collected peak fractions were concentrated by lyophilizing 1000 μ L and reconstituting with 100 μ L 25% (v/v) acetonitrile to afford 10-fold concentrated samples.

Daunorubicin micelle analysis

Stock micellar daunorubicin formulations were prepared at 5 mg/mL total construct in cold saline before AF4 analysis. For plasma incubation studies, sample was prepared at 10 mg/mL total construct in cold saline, and 250 μ L was incubated with 50 μ L human plasma at 37 °C for 2.5 h. Following incubation, the sample was diluted with PBS (200 μ L) before AF4 analysis (5 mg/mL final total construct and 10% (v/v) plasma). The AF4 elution profile employed is given in Table 4. Peak fractions were collected, and fraction volumes measured, before drug content analysis by RP-HPLC.

The RP-HPLC elution gradient was 25% B for 4 min, ramp to 100% B in 8 min, hold at 100% B for 4 min, and ramp down to 25% B in 4 min. Daunorubicin was detected by fluorescence emission at 590 nm (488 nm excitation). Calibration standards (TEVA, Lot No. 6447AO00414R) were prepared

in 25% (v/v) acetonitrile at concentrations ranging from 10–200 ng/mL. Stock injection samples and collected fractions were lyophilized and reconstituted with 25% (v/v) acetonitrile accordingly to fall within the calibration curve range. Typically, 10 μ L stock injection sample was lyophilized and reconstituted accordingly with 25% (v/v) acetonitrile to yield a 1000-fold final diluted sample. Collected peak fractions typically were diluted 2- or 3-fold following reconstitution of the lyophilized fraction.

Doxil analysis

Doxil (Lot 600220P1) was reconstituted according to the manufacturer's instructions. For studies without plasma incubation, the sample was diluted 10-fold in PBS before AF4 analysis. For plasma incubation studies, 100 μ L stock Doxil was incubated with 100 μ L human plasma at 37 °C for 1.5 h. Following incubation, the sample was diluted with PBS (800 μ L) before AF4 analysis (10-fold diluted Doxil and 10% (v/v) plasma). The AF4 elution profile employed is given in Table 5. The chromatographic trace was monitored by DLS detection. Peak fractions were collected, and fraction volumes measured before drug content analysis by RP-HPLC. Doxorubicin RP-HPLC analysis was performed as described previously.

Table 2 AF4 method for the analysis of PEGylated gold nanorods

Step	Δt (min)	Mode	V _x start (mL/min)	V _x end (mL/min)	Focus flow (mL/min)
1	2	Elution	2	2	-
2	2	Focus	-	-	1
3	3	Focus + inject	-	-	1
4	5	Focus	-	-	1
5	50	Elution	2	2	-
6	2	Elution	2	0	-
7	8	Elution	0	0	-
8	2	Elution + inject	0	0	-
9	1	Elution	0	0	-

Table 3 AF4 method for the analysis of doxorubicin and docetaxel liposomes

Step	Δt (min)	Mode	V _x start (mL/min)	V _x end (mL/min)	Focus flow (mL/min)
1	2	Elution	1.5	1.5	-
2	2	Focus	-	-	1
3	5	Focus + inject	-	-	1
4	5	Focus	-	-	1
5	60	Elution	3	0	-
6	10	Elution	0	0	-
7	5	Elution + inject	0	0	-
8	5	Elution	0	0	-

Protein binding assessment

Doxil (Lot 600220P1), Onivyde (Lot 160107), and AmBisome (Lot 010550) were prepared based on their respective prescribing information. For studies without plasma incubation, the samples were diluted 100-fold in PBS before injection into the AF4 system. For plasma incubation studies, 10 μ L of nanoformulation was incubated with 100 μ L human plasma at 37 °C for 2 h. Prior to injection, 890 μ L PBS was added to make the final injection solution 10% (v/v) plasma. The AF4 elution profile employed is given in Table 5. The chromatographic traces were monitored by in-line MALS and DLS detection.

Results and discussion

Herein, several case studies are described which portray the diverse capabilities of AF4 when coupled with other routine analytical techniques. Each case study utilizes distinct nanomedicine formulations, as no single nanoparticle was ideal to showcase the utility of all methods. The section begins with the simplest of applications, analysis of size distribution, and offers a comparison to routine batch-mode DLS. In the subsequent sections, we incorporated offline techniques such as TEM and RP-HPLC to analyze fractions collected from AF4-DLS separation to provide shape and concentration as a function of nanoparticle size. Lastly, incubation in human

plasma is discussed, which provides an estimate of nanoparticle stability and interaction with plasma proteins.

Size distribution

To demonstrate the power of AF4-DLS as a tool for measuring size distribution of nanoparticles, a SN-38-loaded micellar formulation was used. The micellar nanoparticle displayed a very broad peak by batch-mode DLS, with multiple size populations apparent by comparison of the intensity-weighted and volume-weighted size distributions (Fig. 1a). Two overlapping size populations were evident, with the larger size population (roughly 213 nm) dominating the intensity-weighted distribution, and the smaller population (roughly 64 nm) dominating the volume-weighted distribution. This represents a common limitation of batch-mode DLS measurements, namely the limited resolution capacity for nanoparticles that are similar in size. Generally, to achieve good resolution of size populations by batch-mode DLS, the nanoparticle fractions should be a minimum of three times different in size [26].

An AF4 elution profile was developed which teased out the different size populations. The AF4 fractogram, showing DLS and UV detection ($\lambda = 210$ nm), is shown in Fig. 1b. The red trace represents the DLS scattering intensity signal as a function of time. The green dots across the peaks represent the measured Z-average size at each time point. The AF4-DLS fractogram mimics the batch-mode DLS in that two size populations were observed. However, with the AF4-DLS

Table 4 AF4 method for the analysis of daunorubicin micelle

Step	Δt (min)	Mode	V _x start (mL/min)	V _x end (mL/min)	Focus flow (mL/min)
1	2	Elution	1	1	-
2	2	Focus	-	-	1
3	5	Focus + inject	-	-	1
4	10	Focus	-	-	1
5	10	Elution	1	0	-
6	15	Elution	1	0	-
7	15	Elution	0	0	-
8	5	Elution + inject	0	0	-
9	5	Elution	0	0	-

Table 5 AF4 method for the analysis of Doxil, Onivyde, and AmBisome

Step	Δt (min)	Mode	V _x start (mL/min)	V _x end (mL/min)	Focus flow (mL/min)
1	2	Elution	1	1	-
2	2	Focus	-	-	1
3	5	Focus + inject	-	-	1
4	10	Focus	-	-	1
5	10	Elution	1	1	-
6	2	Elution	1	0.5	-
7	50	Elution	0.5	0.5	-
8	2	Elution	0.5	0	-
9	2	Elution	0	0	-
10	2	Elution + inject	0	0	-
11	5	Elution	0	0	-

technique, the broad overlapping size distributions observed in the batch-mode analysis were resolved into two distinct peaks. The nanoparticles eluted from small to large, as expected based on the field flow fractionation (FFF) theory [27]. The first eluting peak was the predominant population as evidenced by its strong UV signal. Its Z-average size distribution ranged 51–99 nm with the lower size, ~ 55 nm, being fairly constant across the peak. This also supported the batch-mode DLS data, whereby the smaller size dominated the volume-weighted distribution, indicating this was the predominant size population. The second, less abundant size population had sizes ranging from 153–248 nm.

Overall, these results demonstrate that AF4, as a separation technique, is capable of resolving broad and polydisperse size populations. When coupled with DLS and UV detection, the size distribution as well as the relative abundance of each population, respectively, can be measured. The AF4-DLS fractogram supports the intensity-weighted batch-mode DLS trace, as both traces showed two populations. AF4-DLS, however, was far superior in separation and resolution of the two populations. Additionally, the AF4-UV fractogram and the volume-weighted batch-mode DLS trace also corresponded very well to each other, both showing the smaller size population as the more abundant species. Although the Z-average size by batch-mode DLS was 119 nm, AF4-DLS-UV was able to discern a 55 nm size population—half that of the batch-mode DLS Z-average size—as the major population in the polydisperse mixture.

Shape distribution

In addition to a population of sizes, various shapes can also be present in a nanoformulation. Batch-mode analysis of PEGylated gold nanorods by DLS showed a single population of 80–90 nm (the ~ 10 nm peak is due to rotational diffusion of the gold nanorods [28]), but was unable to discern different size/shape particles (Fig. 2a). DLS measurement, by default,

assumes a spherical shape for particles, but nonetheless has been used as a first approximation of size for rod-like nanoparticles. Batch-mode analysis by TEM readily identified a mixture of both rod-like and sphere-like particles (Fig. 2b), although it was tedious to approximate a ratio of the two populations. This was only achieved by the time-consuming task of manually counting hundreds-to-thousands of particles over several TEM images.

To separate the various shapes, the PEGylated gold nanorod samples were analyzed via AF4 with both in-line MALS and in-line DLS detectors, and fractions of each peak were collected for analysis by TEM (Fig. 2c–e). Fraction 1 (38–49 min) clearly contained the rod-like particles, while fraction 2 (49–58 min) clearly contained the sphere-like particles based on TEM examination of the separated fractions. While batch-mode DLS was unable to identify two shape populations in the sample, batch-mode TEM easily detected the two shapes. AF4, on the other hand, was able to identify and readily separate the two shape populations. Generally speaking, coupling additional detectors such as UV-Vis or RI would also afford an approximation of the relative ratio of each size/shape population, an attribute not quickly determined by the stand-alone batch-mode techniques.

Further evidence of the shape distribution within each peak was achieved by calculating shape factors for each population. Shape factor can be calculated using the radius of gyration (R_g) obtained from MALS detection and hydrodynamic radius (R_h) obtained from DLS detection. DLS measurement provides a hydrodynamic diameter (D_h), which is converted to R_h to calculate the shape factor ($\rho = R_g/R_h$) for each peak. The shape factor for ideal hard spheres approaches the value $(3/5)^{1/2} \approx 0.77$ [22]. As the mass distribution is centered towards the core of the sphere, the shape factor decreases, and as the mass distribution shifts towards the exterior of the sphere, the shape factor increases. Shape factor values greater than ~ 1.22 generally suggest a rod-like geometry [23]. The calculated shape factor for peak 1 was 2.4, affirming rod-like particles,

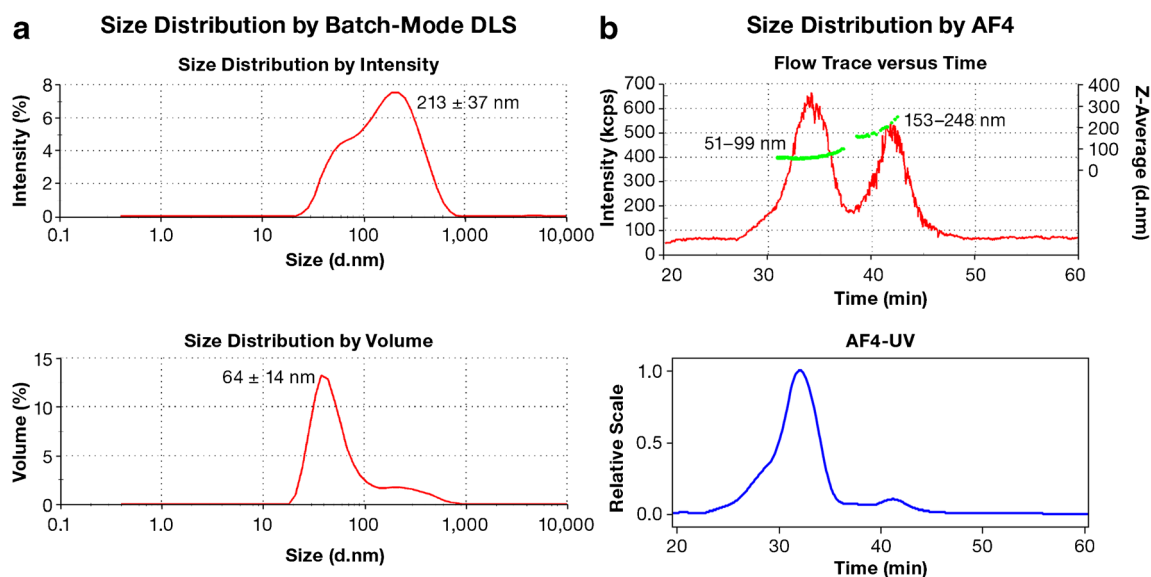


Fig. 1 Size distribution by batch-mode DLS vs. AF4-DLS. **(a)** Batch-mode intensity- (top) and volume-weighted (bottom) DLS distributions for SN-38-loaded micelles. Measurements were made after a 10-fold dilution in PBS and at 25 °C. The average intensity- and volume-weighted sizes are noted. **(b)** Flow-mode AF4 separation with in-line

DLS (top) and UV detection at 210 nm (bottom) for SN-38-loaded micelles. The hydrodynamic size was measured across the peaks (green squares) using a Malvern Zetasizer and was based on an intensity threshold of > 200 kcps. The Z-average size distribution for each peak is noted.

while the calculated shape factor for peak 2 was 1.0, supporting the finding of sphere-like particles. Using simple shape factor calculations, AF4-MALS-DLS alone was able to provide information on the shape of the two separated populations, supporting the TEM data.

Drug distribution

With polydisperse formulations, it can be imperative to understand the drug loading, or drug distribution across the various size populations. Drugs may preferentially load into one or more size populations in a mixture. Having this information at an early stage of development can allow for optimization of the formulation and elimination of populations without cargo. To highlight this AF4 capability, a dual drug-loaded liposome was used, containing both doxorubicin and docetaxel.

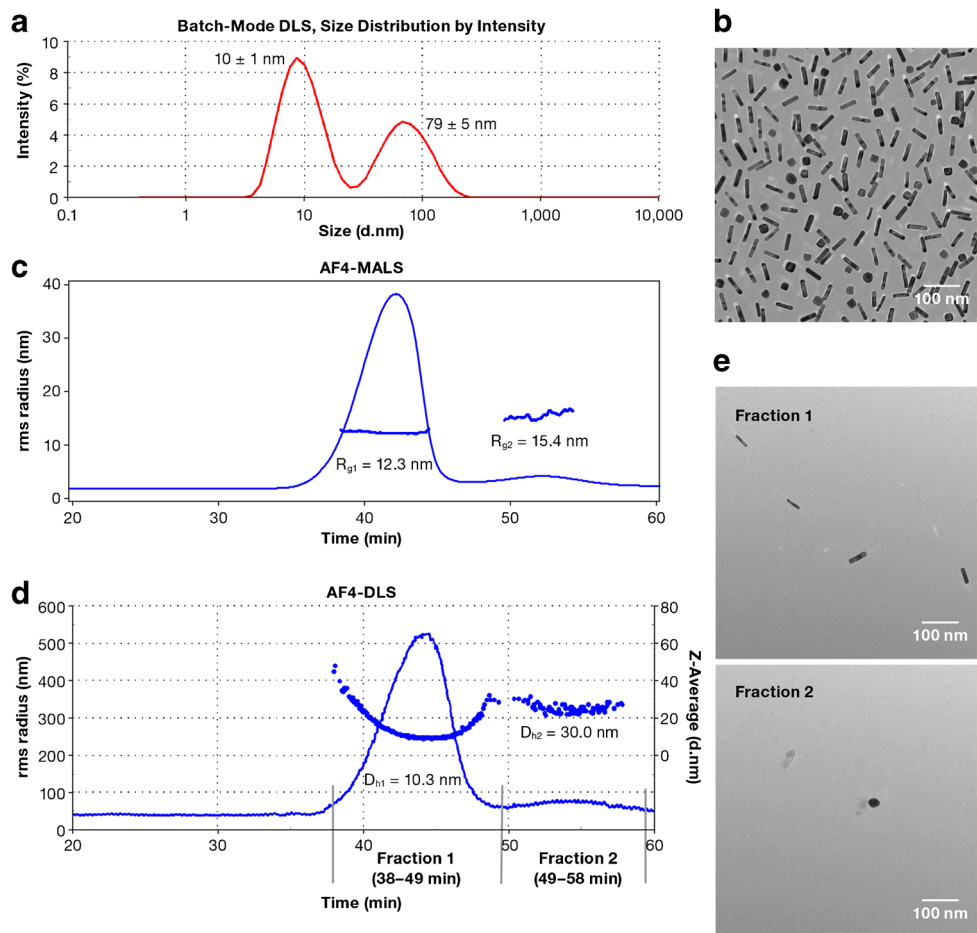
The AF4 fractogram for the dual drug-loaded liposome is depicted in Fig. 3. Two major peaks were present. The first peak was broad and showed two clear size trends by DLS. The first was a population with a near constant size of approx. 30 nm, while the second showed a population with a range of sizes spanning 35–108 nm. The second peak in the fractogram contained larger liposomes spanning 104–274 nm. The utility of AF4 was expanded by collecting fractions for subsequent analysis by RP-HPLC to determine the drug loading in each of the populations present in the mixture.

Fractions were collected for each of the three noted size populations, as well as the elution period between the two peaks (denoted by solid gray vertical lines in the fractogram). Each fraction was analyzed by RP-HPLC for doxorubicin and

docetaxel content using either fluorescence or UV detection, respectively. Fractions were collected manually, volumes measured, then lyophilized, and reconstituted accordingly before drug concentration analysis. The majority of the recovered doxorubicin was measured in peak 1, fractions 1 and 2. Approximately 19% of the total injected doxorubicin was detected in the ~30 nm population (fraction 1), while double that amount was in the latter part of peak 1, wherein the sizes spanned 35–108 nm. A small percentage was recovered in peak 2 (fraction 4) with the larger sized liposome population (104–274 nm), as well as in the elution period between peaks 1 and 2 (fraction 3). Thus, the majority of the doxorubicin resided in the smaller size liposome population. Knowing the drug distribution across various size populations in a formulation can provide insight into preferential loading for a specific size and can be used to optimize the formulation's production process.

The total drug recovery for doxorubicin was 64% of the injected amount. In contrast, there was very little recovery of the docetaxel. Approximately 6% was recovered in the ~30 nm population (fraction 1) and only 1% in the 35–108 nm population (fraction 2) of peak 1. There was no detectable docetaxel recovery in fractions 3 or 4. The differences in total drug recovery are directly related to the loading of the drugs within the liposome. Notably, doxorubicin is loaded into the interior hydrophilic core of the liposome, while docetaxel is loaded into the lipid bilayer. It is hypothesized that docetaxel, a very hydrophobic drug, likely partitioned from the liposomes to the BSA on the AF4 membrane. Drugs that reside in the lipid bilayer of liposomes can be more prone to release

Fig. 2 Shape distribution using AF4-DLS-TEM. **(a)** Batch-mode intensity-weighted DLS distribution for PEGylated gold nanorods. Measurements were made after a 10-fold dilution in PBS and at 25 °C. **(b)** Batch-mode TEM image. **(c)** Flow-mode AF4 separation with in-line MALS detection. The R_g for each population is noted in the figure. **(d)** Flow-mode AF4 separation with in-line DLS. The hydrodynamic size was measured across the peaks (blue squares) using a Malvern Zetasizer and was based on an intensity threshold of > 65 kcps. The Z-average size distribution for each peak is noted. **(e)** TEM images of each population isolated after AF4 separation.



by partitioning to proteins bound to the AF4 membrane or even membranes of larger size (e.g., larger liposomes, red blood cells). Assessing stability of nanoparticles, in terms of drug release, is described in more detail in the next case study.

Nanoparticle stability

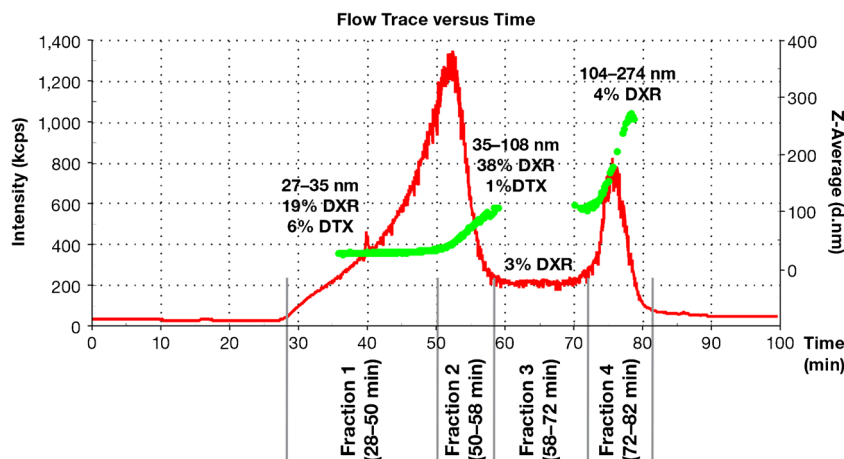
AF4 can also be used as a rapid tool to assess the stability of a formulation, and notably can be tested in a biological matrix. Using the above-described AF4-DLS-RP-HPLC technique, a micellar formulation of daunorubicin [25] was analyzed and the drug across the nanoparticle peak quantitated. The resulting AF4-DLS fractogram is depicted in Fig. 4a. Fractions were collected after the focusing step (20 min) until the end of the run (69 min) as denoted by solid gray vertical lines along the corresponding elution times, for a total of five fractions. The first fraction was 1 min after the focusing step and contained any quickly eluting micelles which were not focused (cross-flow rate was 1 mL/min). The second and third fractions corresponded to a linear decrease in the cross-flow rate from 1 to 0 mL/min and contained the major population of nanoparticles. The fourth fraction corresponded to a cross-flow rate of 0 mL/min and would

contain any larger micelles that may have been pinned against the membrane. The fifth fraction corresponded to the cleaning of the sample loop, where the sample loop is opened and flushed prior to the next run.

The size distribution and drug concentration for each collected fraction is noted in Fig. 4a. The micelle eluted as a single peak but with two distinct size trends as measured by flow-mode DLS. The majority of this peak contained nanoparticles of a fairly constant size range, with Z-average sizes between 34 and 52 nm (fraction 2). This peak also contained the majority of the drug, 24% of the total recovered drug. The second half of this peak showed an increase in size, up to 103 nm, and contained an additional 12% of the total recovered drug (fraction 3). Small quantities of drug, 4%, were also distributed among the fractions collected before and after the main peak (fractions 1 and 4), and the sample loop cleaning peak (fraction 5). While a very small light scattering signal was observed for fraction 5 (~ 61 min), no measurable size was detected, likely due to low concentration.

Note the total amount of drug recovered across all peaks was only 40% relative to the amount injected. This result was consistent and reproducible. There are several possible causes for the low drug recovery: (1) sample loss due to membrane

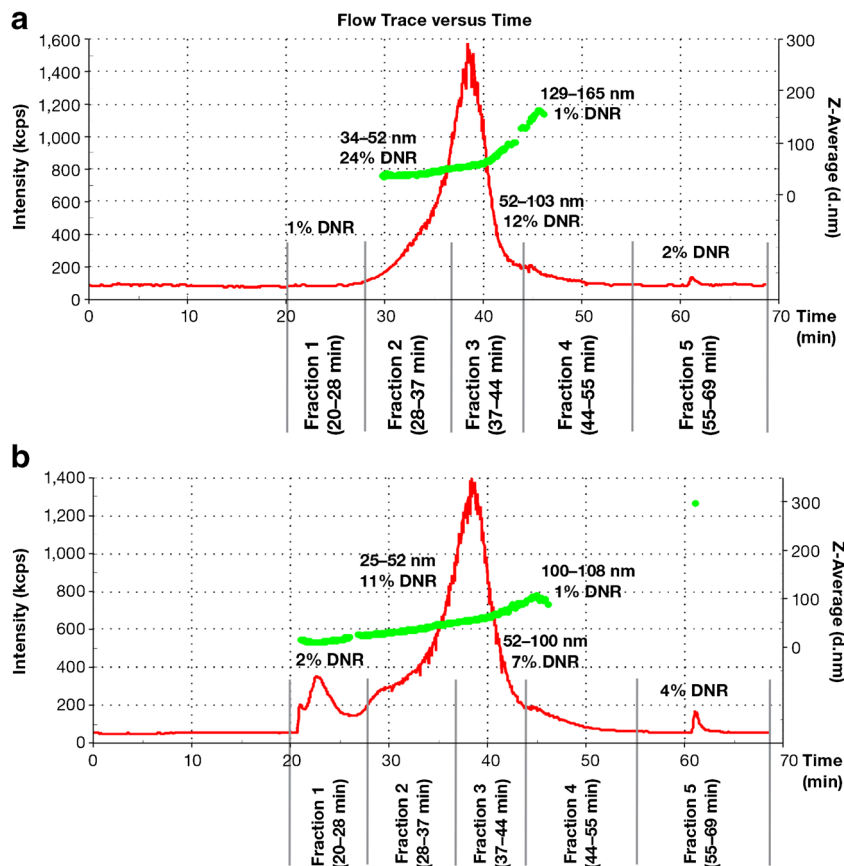
Fig. 3 Drug loading with respect to size distribution using AF4-DLS-RP-HPLC. Flow-mode AF4 separation with in-line DLS for doxorubicin (DXR)- and docetaxel (DTX)-loaded liposomes. The hydrodynamic size was measured across the peaks (green squares) using a Malvern Zetasizer and was based on an intensity threshold of > 240 kcps. The Z-average size distribution and the percent drug recovery relative to the total amount injected are given for each fraction.



sticking, (2) incomplete peak/fraction collection, (3) drug is free/unassociated with the nanoparticle, or (4) drug loss through some alternative mechanism. Sample (micelle) loss to membrane sticking is minimized by passivating the membrane with bovine serum albumin (BSA) per the instrument manufacturer's (Wyatt) recommendations. BSA was run through the system three times prior to sample injection. Nanoparticles which are surface modified with hydrophilic coatings, e.g., PEGylated in this case, should also aid in minimizing membrane interactions. Collecting fractions across

the entire run, as done here, essentially eliminates the possibility of drug loss due to incomplete collection and should recover all drug injected, provided it is associated with the nanoparticle. Any free drug present in the system, however, would not be recovered. It would either pass through the membrane (10 kDa molecular weight cutoff, MWCO) or bind to the BSA passivated on the membrane. In this example, the free daunorubicin amount was measured beforehand using centrifugal filtration and RP-HPLC analysis and was < 5% (data not shown). Passivation of the membrane, PEGylation

Fig. 4 Nanoparticle drug recovery pre- and post-plasma incubation. Flow-mode AF4 separation of daunorubicin-loaded micelles with in-line DLS (a) pre- and (b) post-incubation with human plasma. The hydrodynamic size was measured across the peaks (green squares) using a Malvern Zetasizer and was based on an intensity threshold of > 150 kcps. The size ranges are given in the figure for each peak. Collected fractions are designated by solid gray vertical lines along with the elution times. The percent daunorubicin drug recovery relative to the total amount injected is given for each fraction.



of the surface, collection of peaks throughout the entire run, and low free drug in the system all help to minimize drug loss in the AF4 system, suggesting there may be another underlying mechanism responsible for the poor drug recovery.

One hypothesis is the daunorubicin partitions from the micelles to the BSA on the membrane. In this case, daunorubicin would not be recovered and could explain the low total drug recovery. This data suggests that daunorubicin is unstable in the micellar formulation and is released from the formulation in the presence of BSA. As serum albumin accounts for more than 50% of the protein in plasma, this suggests the formulation would be unstable in biological matrix as well and release the majority of drug almost immediately. To test this hypothesis, the daunorubicin micelles were incubated in plasma prior to injection into the AF4 system.

The micelles were incubated in human plasma at 37 °C for a minimum of 2 h. The samples were then diluted with PBS after incubation to achieve a suitable DLS signal and a final plasma concentration of 10% (v/v). Higher final plasma concentrations tend to foul and clog the AF4 system faster. As before, fractions were collected after the focusing step until the end of the run to maximize total drug recovery. Collecting fractions for the entirety of the AF4 elution also aids in total mass recovery calculations, which is especially important when assessing the stability of the nanoformulation. Fractions were then analyzed for drug content by RP-HPLC.

The AF4-DLS fractogram after plasma incubation is shown in Fig. 4b and was similar to the non-plasma incubated fractogram in Fig. 4a, with the exception of an additional peak in fraction 1 at approx. 23 min. This peak corresponds to plasma proteins (e.g., albumins, globulins, and fibrinogens). As with the previous fractogram, the major nanoparticle population spanned fractions 2 and 3. Fraction 2 again had a narrower, more constant size range and contained the largest fraction of recovered drug. Fraction 3 showed an increasing size population and contained the second largest fraction of recovered drug. Combined, fractions 2 and 3 recovered 18% of the total injected drug in the plasma incubation, only half of the recovered 36% (in fractions 2 and 3) for the sample without plasma incubation. A slight increase in the amount of drug present in fraction 1 (2%) is attributed to drug binding to the protein. There was also an increase of drug detected in fraction 5 (4%). This is likely due to elution of additional proteins with bound drug in the sample loop cleaning step. The total amount of drug recovered across all the peaks was 25% relative to the amount injected, nearly half of the 40% recovered without plasma incubation. This confirms further instability/release of free drug in the presence of plasma. We speculate the drug partitions to the plasma proteins during incubation, and as the sample flows across the AF4 membrane, there is additional partitioning of the drug from the plasma proteins to the BSA passivated on the membrane and/or plasma protein exchange/further passivation of the membrane. In a separate run, the

AF4 membrane was passivated with 10% human plasma in lieu of BSA to ascertain whether any differences in protein composition would affect drug partitioning. However, the results were the same (data not shown) as those obtained through the BSA-passivated membrane.

To ensure the poor drug recovery was a result of nanoparticle instability (facile drug release) and not an artifact of the process, this was repeated using Doxil. Doxil is a stable, controlled release liposomal formulation of doxorubicin. AF4-DLS fractograms of Doxil pre- and post-incubation in human plasma are shown in Fig. 5. Three fractions were collected, 1 min after the focusing step, the main nanoparticle peak elution, and the sample loop cleaning step. The DLS measured size and recovered doxorubicin content for each are noted in the figure. There was 82% drug recovery in the main peak (fraction 2) and 5% drug recovery in sample loop cleaning step (fraction 3) for the non-plasma incubated sample. There was essentially no change in drug recovery after plasma incubation, with 80% and 5% recovery for fractions 2 and 3, respectively. This demonstrates that nanomaterials with stably encapsulated drugs show a good drug recovery by AF4-RP-HPLC and drug is not lost as a result of the procedure itself.

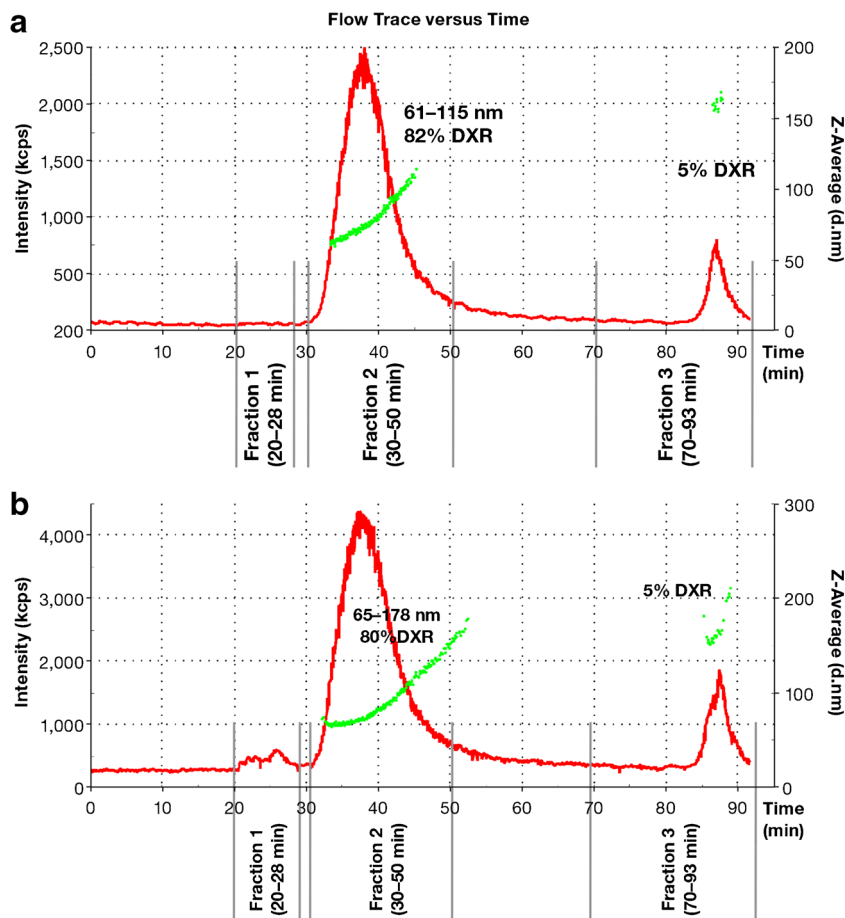
Nanoparticle incubation experiments in plasma, coupled with AF4-DLS-RP-HPLC analysis, can provide insight into the stability of the nanoparticle, with respect to drug release, providing a quick method to qualitatively assess the stability of a formulation in physiologically relevant matrix. For many formulations, AF4-DLS-RP-HPLC analysis without plasma incubation may also allude to the stability issue, allowing for elimination of the plasma incubation step. Indeed, in the case of the daunorubicin micelle, less than half of the total injected drug was recovered without plasma incubation, hinting at the possibility of instability. A further reduction in drug recovery upon plasma incubation reaffirmed this notion. However, not all formulations may show drug loss via AF4 separation alone, making plasma incubation a great addend to nanoparticle stability assessment, especially for nanomedicine applications.

Assessment of protein binding

In addition to gauging nanoparticle stability, plasma incubation studies are also a useful tool for assessing protein binding. Numerous studies have demonstrated that surface modification with polyethylene-glycol (PEG) or similar hydrophobic moieties minimizes protein binding, which can inhibit uptake by the mononuclear phagocyte system (MPS) and significantly prolong circulation times, thus improving bioavailability [29–31]. This technique proves useful in detecting protein binding and characterizing the extent of protein interactions with nanoparticles.

In this study, three commercially available liposomes were investigated: Doxil, Onivyde, and AmBisome. Each liposomal formulation contains a different degree of surface

Fig. 5 Nanoparticle drug recovery pre- and post-plasma incubation. Flow-mode AF4 separation of Doxil (doxorubicin-loaded liposomes) with in-line DLS (a) pre- and (b) post-incubation with human plasma. The hydrodynamic size was measured across the peaks (green squares) using a Malvern Zetasizer and was based on an intensity threshold of > 600 kcps. The size ranges are given in the figure for each peak. Collected fractions are designated by solid gray vertical lines along with the elution times. The percent doxorubicin drug recovery relative to the total amount injected is given for each fraction.



PEGylation through incorporation of PEG-derivatized lipids into the liposome bilayer. The three samples were analyzed via AF4 with both in-line MALS and in-line DLS detectors. Samples were run pre- and post-incubation in plasma as described earlier, and the size of the nanoparticle peaks measured by both MALS and DLS to provide the R_g and D_h , respectively, which were used to calculate the shape factor. The shape factors pre- and post-incubation in plasma were then compared for an assessment of protein binding.

Doxil, a liposomal doxorubicin formulation, contains 2 mg/mL of doxorubicin, 3.19 mg/mL of N-(carbonylmethoxypolyethylene glycol 2000)-1,2-distearoyl-sn-glycero-3-phosphoethanolamine sodium salt (DSPE-mPEG2000), 9.58 mg/mL of fully hydrogenated soy phosphatidylcholine (HSPC), and 3.19 mg/mL of cholesterol, which gives ~5% molar ratio of PEGylation [32]. As shown in Fig. 6a, the AF4-MALS-DLS results showed that Doxil, without incubation in plasma, had an average R_g of 37.6 nm (range from 25–50 nm), and an average D_h of 93.9 nm (range from 50 to 120 nm). The calculated shape factor (ρ) was 0.8, which indicated a uniform spherical shape for the liposome. After incubation with human plasma, the average R_g remained the same, at 37.8 nm (range from 25–50 nm), and the average D_h was 97.9 nm (range from 45–140 nm). The calculated shape

factor after plasma incubation was 0.8, again indicating a uniform spherical shape. There was no significant shift in shape factor compared with the pre-plasma incubation. This data indicates that under a high protein concentration (plasma incubation), Doxil had minimal protein binding on the surface.

Onivyde is a commercially available liposomal dispersion containing irinotecan. Onivyde contains 4.3 mg/mL irinotecan free base, 6.81 mg/mL of 1,2-distearoyl-sn-glycero-3-phosphocholine (DSPC), 2.22 mg/mL of cholesterol, and 0.12 mg/mL of DSPE-mPEG2000, which gives ~0.3% molar ratio of PEGylation, about one-tenth the PEGylation of Doxil [33]. Onivyde showed an average R_g of 51.8 nm (range from 30–65 nm), and average D_h 120.5 nm (range from 50–150 nm) (Fig. 6b). Using these measured values, the shape factor was calculated to be 0.9. After incubation with plasma, the shape factor of Onivyde increased to 1.0. This shift in shape factor was the result of a decrease in the measured D_h value. After incubation with plasma, the D_h shifted from 120.5 to 108.4 nm (range from 45–140 nm). The increased shape factor indicates a mass distribution shift to the surface of the liposomes, suggesting protein binding on the surface.

The third test sample in this case study was AmBisome, a liposomal formulation of amphotericin B. AmBisome contains 4 mg/mL amphotericin B, 17.75 mg/mL of HSPC,

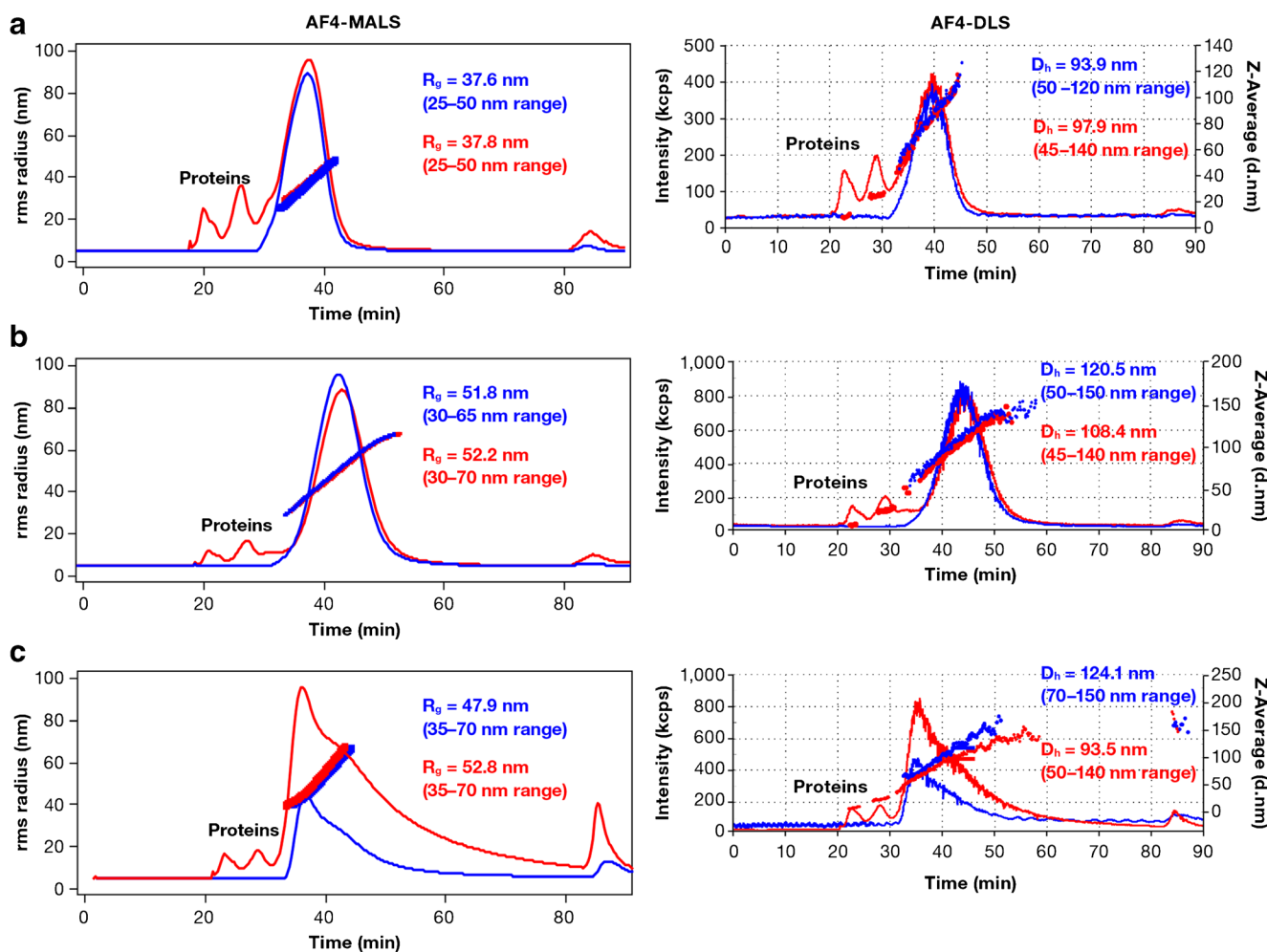


Fig. 6 Assessment of protein binding. Flow-mode AF4 separation of (a) Doxil, (b) Onivyde, and (c) AmBisome using both MALS (left panels) and DLS (right panels) detection. The blue traces represent nanoparticles without plasma incubation. The red traces represent nanoparticles with plasma incubation. The radius of gyration (R_g) and hydrodynamic diameter (D_h) from MALS and DLS, respectively, are given in the figures. The

intensity thresholds for DLS were manually adjusted for each experiment. The intensity thresholds without plasma incubation were > 65, > 50, and > 100 kcps for Doxil, Onivyde, and AmBisome, respectively. The intensity thresholds with plasma incubation were > 130, > 130, and > 120 kcps, respectively.

4.33 mg/mL of cholesterol, and 7.00 mg/mL of distearoyl phosphatidylglycerol [34]. It is formulated as a single bilayer liposomal drug delivery system with no PEGylation on the surface. Before incubation with plasma, AmBisome had a R_g value of 47.9 nm (range from 35–70 nm) and a D_h value of 124.1 nm (range from 70–150 nm) (Fig. 6c). The resulting shape factor was 0.8, indicative of a uniform spherical shape. After incubating with plasma, the R_g value increased to 52.8 nm (range from 35–70 nm) and the D_h value decreased to 93.5 nm, resulting in an increase in the shape factor to 1.1. This increased shape factor, again, indicates a mass distribution shift to the surface of the liposomes, suggesting protein binding on the surface. The shape factor for AmBisome after plasma incubation was larger than that observed with Onivyde plasma incubation. Also of note was a significant broadening of the nanoparticle peak, which was not observed for Doxil or Onivyde, as well as a significant increase in the intensity of the

peak. Both the shape factor and the peak changes suggest a substantial amount of protein binding on the liposome and concur with the expected results for a non-PEGylated liposomal formulation.

All three commercially available nanoformulations showed comparable hydrodynamic diameters (~ 90–120 nm) despite various degrees of PEGylation. Under high protein concentration (10% human plasma), Doxil, with 5% (molar ratio) PEGylation, showed no change in shape factor, suggesting minimal protein binding. For Onivyde, the shape factor increased ~ 12% due to a relatively low percentage of PEGylation (0.3% molar ratio) which afforded some protein binding to the surface. AmBisome, on the other hand, which contains no PEG, showed a significant increase in shape factor (41%) and significant changes to the overall peak shape. The mass shift towards the surface of the liposome (as indicated by the shape factor) and the increased peak intensity and width

indicate substantial protein binding. Certainly, differences in the lipid composition, namely PEG content, contribute to the protein binding capacity of the formulations. It also noted that the nanoformulations differ in terms of their drug loading. Both Doxil and Onivyde are interior loaded liposomes with the drug inside the hydrophilic core, while amphotericin B is intercalated within the unilamellar bilayer liposome membrane in AmBisome. While these differences could contribute to the stability of the nanoformulation under AF4 flow-mode separation, which may lead to changes in peak size or shape, the protein binding capacity of each formulation as assessed by changes in shape factor aligned with the expected results for PEGylated vs. non-PEGylated nanomedicines.

Overall, AF4-MALS-DLS analysis proved to be a quick method to qualitatively assess nanoparticle protein binding and gauge the interaction of nanoparticles with plasma proteins. Such information could be helpful in the rational design of formulations, wherein protein binding is a critical component of the biological performance of systemically administered nanomedicines.

Conclusions

Size and shape distribution, drug loading, stability in physiological matrix, and protein binding capacity are all important characteristics for nanomedicine formulations. Size, shape, and protein binding can influence biodistribution, off-target toxicities, and ultimately efficacy. Drug loading is imperative for correct dosing. And, formulations that are not stable in physiological matrix can be expected to release drug prematurely, before reaching the intended site of action. AF4 coupled with other routine analytical techniques has been shown to be a versatile tool to assess each of these characteristics and can be a valuable asset during early preclinical development and testing of nanomedicines.

AF4 coupled with in-line DLS detection was shown to provide enhanced resolution of similarly sized populations in polydisperse mixtures versus the often utilized batch-mode DLS technique. By further adding RP-HPLC analysis, the drug distribution across the various size populations can be also measured. Although drug loading was the only compositional aspect discussed herein, this could be readily extended to other components of a nanomaterial, including targeting ligands. Moreover, other techniques, such as TEM [20], inductively coupled plasma mass spectrometry (ICP-MS) [7, 35, 36], and resistive pulse sensing and more [10, 37], can be applied to AF4 fractions for information on particle shape, morphology, impurities, and concentration, affording superior insight into the make-up of each population.

AF4 also provides another advantage many other analytical techniques do not by allowing for analysis in plasma. The ability to rapidly and easily evaluate the characteristics of a

nanomedicine in biological matrix is an invaluable advantage. Traits such as stability and protein binding are often difficult and/or time consuming to assess using traditional approaches [38]. Using AF4-DLS coupled with RP-HPLC analysis, drug recoveries can be measured pre- and post-incubation in plasma to assess formulation stability, while AF4-MALS-DLS can be used to calculate shape factors pre- and post-incubation with plasma. Shape factors are a good indicator of protein binding by monitoring for mass shifts at the surface of the particle.

The techniques presented here serve to address critical questions pertaining to the overall suitability of a nanomedicine. Furthermore, they are relatively simple and quick, and can identify potential concerns at an early stage, facilitating the overall development and optimization process.

Acknowledgements The authors are grateful to Intezyme Technologies, Inc., Siva Therapeutics, and Cureport, Inc., for generously providing samples. The authors thank Joseph Meyer, Leidos Biomedical Research, Inc., for graphic illustrations.

Funding information This project has been funded in whole or in part with federal funds from the National Cancer Institute, National Institutes of Health, under Contract No. HHSN261200800001E.

Compliance with ethical standards For plasma incubation studies, human plasma was collected from healthy volunteer donors under National Cancer Institute (NCI) at Frederick Protocol OH99-C-N046.

Conflict of interest The authors declare that they have no competing interests.

Disclaimer The content of this publication does not necessarily reflect the views or policies of the Department of Health and Human Services, nor does mention of trade names, commercial products, or organizations imply endorsement by the US Government.

References

1. D'Mello SR, Cruz CN, Chen M-L, Kapoor M, Lee SL, Tyner KM. The evolving landscape of drug products containing nanomaterials in the United States. *Nat Nanotechnol.* 2017;12:523.
2. Maguire CM, Rösslein M, Wick P, Prina-Mello A. Characterisation of particles in solution – a perspective on light scattering and comparative technologies. *Sci Technol Adv Mater.* 2018;19(1):732–45.
3. Anderson W, Kozak D, Coleman VA, Jamting AK, Trau M. A comparative study of submicron particle sizing platforms: accuracy, precision and resolution analysis of polydisperse particle size distributions. *J Colloid Interface Sci.* 2013;405:322–30.
4. Varenne F, Makky A, Gaucher-Delmas M, Violleau F, Vauthier C. Multimodal dispersion of nanoparticles: a comprehensive evaluation of size distribution with 9 size measurement methods. *Pharm Res.* 2016;33(5):1220–34.
5. Caputo F, Clogston J, Calzolari L, Rösslein M, Prina-Mello A. Measuring particle size distribution of nanoparticle enabled medicinal products, the joint view of EUNCL and NCI-NCL. A step by step approach combining orthogonal measurements with increasing complexity. *J Control Release.* 2019;299:31–43.

6. Gioria S, Caputo F, Urban P, Maguire CM, Bremer-Hoffmann S, Prina-Mello A, et al. Are existing standard methods suitable for the evaluation of nanomedicines: some case studies. *Nanomedicine* (London). 2018;13(5):539–54.
7. Contado C. Field flow fractionation techniques to explore the “nano-world”. *Anal Bioanal Chem*. 2017;409(10):2501–18.
8. Giddings JC. Field-flow fractionation: analysis of macromolecular, colloidal, and particulate materials. *Science*. 1993;260(5113):1456–65.
9. Kowalkowski T, Buszewski B, Cantado C, Dondi F. Field-flow fractionation: theory, techniques, applications and the challenges. *Crit Rev Anal Chem*. 2006;36(2):129–35.
10. Wagner M, Holzschuh S, Traeger A, Fahr A, Schubert US. Asymmetric flow field-flow fractionation in the field of nanomedicine. *Anal Chem*. 2014;86(11):5201–10.
11. Edwards KA, Baeumner AJ. Analysis of liposomes. *Talanta*. 2006;68(5):1432–41.
12. Moon MH, Giddings JC. Size distribution of liposomes by flow field-flow fractionation. *J Pharm Biomed Anal*. 1993;11(10):911–20.
13. Roda B, Zattoni A, Reschiglian P, Moon MH, Mirasoli M, Michelini E, et al. Field-flow fractionation in bioanalysis: a review of recent trends. *Anal Chim Acta*. 2009;635(2):132–43.
14. Messaud FA, Sanderson RD, Runyon JR, Otte T, Pasch H, Williams SKR. An overview on field-flow fractionation techniques and their applications in the separation and characterization of polymers. *Prog Polym Sci*. 2009;34(4):351–68.
15. Zattoni A, Roda B, Borghi F, Marassi V, Reschiglian P. Flow field-flow fractionation for the analysis of nanoparticles used in drug delivery. *J Pharmaceut Biomed*. 2014;87:53–61.
16. Cho TJ, Hackley VA. Fractionation and characterization of gold nanoparticles in aqueous solution: asymmetric-flow field flow fractionation with MALS, DLS, and UV-Vis detection. *Anal Bioanal Chem*. 2010;398(5):2003–18.
17. Hansen M, Smith MC, Crist RM, Clogston JD, McNeil SE. Analyzing the influence of PEG molecular weight on the separation of PEGylated gold nanoparticles by asymmetric-flow field-flow fractionation. *Anal Bioanal Chem*. 2015;407(29):8661–72.
18. Gigault J, Cho TJ, MacCuspie RI, Hackley VA. Gold nanorod separation and characterization by asymmetric-flow field flow fractionation with UV-Vis detection. *Anal Bioanal Chem*. 2013;405(4):1191–202.
19. Nguyen TM, Gigault J, Hackley VA. PEGylated gold nanorod separation based on aspect ratio: characterization by asymmetric-flow field flow fractionation with UV-Vis detection. *Anal Bioanal Chem*. 2014;406(6):1651–9.
20. Chuan YP, Fan YY, Lua L, Middelberg AP. Quantitative analysis of virus-like particle size and distribution by field-flow fractionation. *Biotechnol Bioeng*. 2008;99(6):1425–33.
21. Mathaes R, Winter G, Engert J, Besheer A. Application of different analytical methods for the characterization of non-spherical micro- and nanoparticles. *Int J Pharm*. 2013;453(2):620–9.
22. Burchard W, Schmidt M, Stockmayer WH. Information on polydispersity and branching from combined quasi-elastic and integrated scattering. *Macromolecules*. 1980;13:1265–72.
23. Tande BM, Wagner NJ, Mackay ME, Hawker CJ, Jeong M. Viscosimetric, hydrodynamic, and conformational properties of dendrimers and dendrons. *Macromolecules*. 2001;34(24):8580–5.
24. Carie A, Rios-Doria J, Costich T, Burke B, Slama R, Skaff H, et al. IT-141, a polymer micelle encapsulating SN-38, induces tumor regression in multiple colorectal cancer models. *J Drug Deliv*. 2011;2011:869027.
25. Costich TL, Carie A, Semple JE, Sullican B, Vojtkovsky T, Ellis T, et al. IT-143, a polymer micelle nanoparticle, widens therapeutic window of daunorubicin. *Pharm Nanotechnol*. 2016;4(1):3–15.
26. Clogston JD, Crist RM, McNeil SE. Physicochemical characterization of polymer nanoparticles: challenges and present limitations. In: Vauthier C, Ponchel G, editors. *Polymer nanoparticles for nanomedicines: a guide for their design, preparation and development*. Cham: Springer International Publishing; 2016. p. 187–203.
27. Podzimek S. Asymmetric flow field flow fractionation. In: *Light scattering, size exclusion chromatography and asymmetric flow field flow fractionation: powerful tools for the characterization of polymers, proteins and nanoparticles*: John Wiley & Sons, Inc; 2011. p. 259–305.
28. Clogston JD, Patri AK. Importance of physicochemical characterization prior to immunological studies. *Handbook of Immunological Properties of Engineered Nanomaterials*; 2013. 1:25-52.
29. Dos Santos N, Allen C, Doppen AM, Anantha M, Cox KA, Gallagher RC, et al. Influence of poly(ethylene glycol) grafting density and polymer length on liposomes: relating plasma circulation lifetimes to protein binding. *Biochim Biophys Acta*. 2007;1768(6):1367–77.
30. Digiaco L, Pozzi D, Amenitsch H, Caracciolo G. Impact of the biomolecular corona on the structure of PEGylated liposomes. *Biomater Sci-Uk*. 2017;5(9):1884–8.
31. Bartucci R, Pantusa M, Marsh D, Sportelli L. Interaction of human serum albumin with membranes containing polymer-grafted lipids: spin-label ESR studies in the mushroom and brush regimes. *Biochim Biophys Acta*. 2002;1564(1):237–42.
32. Doxil package insert. <http://www.janssenlabels.com/package-insert/product-monograph/prescribing-information/DOXIL-pi.pdf>.
33. Onivyde package insert. https://www.ipsen.com/websites/Ipsen_Online/wp-content/uploads/sites/9/2019/01/21083350/ONIVYDE_USPI.pdf.
34. AmBisome prescribing information. <https://www.astellas.us/docs/ambisome.pdf>.
35. Beckett R, Giddings JC. Entropic contribution to the retention of nonspherical particles in field-flow fractionation. *J Colloid Interface Sci*. 1997;186(1):53–9.
36. Dubascoux S, Le Hecho I, Hasseloev M, Von de Krammer F, Gautier MP, Lespes G. *Anal At Spectrom*. 2010;25:613–23.
37. Makan AC, Sinha P, Ngaza N, van Aswegen W, Pasch H. Asymmetrical flow field-flow fractionation as a novel technique for the analysis of PS-b-PI copolymers. *Anal Bioanal Chem*. 2013;405(28):9041–7.
38. Dobrovolskaia MA, Neun BW, Man S, Ye X, Hansen M, Patri AK, et al. Protein corona composition does not accurately predict hemato-compatibility of colloidal gold nanoparticles. *Nanomed Nanotechnol Biol Med*. 2014;10(7):1453–63.

Publisher's note Springer Nature remains neutral with regard to jurisdictional claims in published maps and institutional affiliations.